Journal of Quantitative Spectroscopy & Radiative Transfer 113 (2012) 715–720

Contents lists available at SciVerse ScienceDirect

Journal of Quantitative Spectroscopy & Radiative Transfer

journal homepage: www.elsevier.com/locate/jqsrt

On spectral invariance of single scattering albedo for water droplets and ice crystals at weakly absorbing wavelengths

Alexander Marshak [a,*], Yuri Knyazikhin [b], J. Christine Chiu [c], Warren J. Wiscombe [a]

[a] NASA Goddard Space Flight Center, code 613, Greenbelt, MD 20771, USA
[b] Boston University, 675 Commonwealth Avenue, Boston, MA 02215, USA
[c] Department of Meteorology, University of Reading, Reading, UK

ARTICLE INFO

Article history:
Received 2 December 2011
Received in revised form
11 February 2012
Accepted 13 February 2012
Available online 18 February 2012

Keywords:
Single scattering albedo
Droplets
Ice particles
Spectral invariance

ABSTRACT

The single scattering albedo $\omega_{0\lambda}$ in atmospheric radiative transfer is the ratio of the scattering coefficient to the extinction coefficient. For cloud water droplets both the scattering and absorption coefficients, thus the single scattering albedo, are functions of wavelength λ and droplet size r. This note shows that for water droplets at weakly absorbing wavelengths, the ratio $\omega_{0\lambda}(r)/\omega_{0\lambda}(r_0)$ of two single scattering albedo spectra is a linear function of $\omega_{0\lambda}(r)$. The slope and intercept of the linear function are wavelength independent and sum to unity. This relationship allows for a representation of any single scattering albedo spectrum $\omega_{0\lambda}(r)$ via one known spectrum $\omega_{0\lambda}(r_0)$. We provide a simple physical explanation of the discovered relationship. Similar linear relationships were found for the single scattering albedo spectra of non-spherical ice crystals.

Published by Elsevier Ltd.

1. Introduction and the main result

The single scattering albedo in atmospheric radiative transfer is the ratio of the scattering coefficient to the extinction coefficient (e.g., [4], p. 257). It is equal to unity if all extinction is due to scattering (e.g., Rayleigh molecular scattering); conversely, it is equal to zero if all extinction is due to absorption (e.g., gaseous absorption). For spherical particles with a homogeneous refractive index single scattering albedo is calculated using Mie theory. For cloud water droplets both the scattering and absorption coefficients, thus the single scattering albedo, are functions of wavelength and droplet size. If the distribution of droplet sizes is given, both the coefficients and the single scattering albedo can be determined as functions of effective radius provided that the width of the droplet size distribution is constant.

In general, the single scattering albedo ω_0, as a function of effective radius r and wavelength λ, is defined as

$$\omega_{0\lambda}(r)=\frac{\sigma_{s\lambda}(r)}{\sigma_{s\lambda}(r)+\sigma_{a\lambda}(r)} \tag{1}$$

where $\sigma_{s\lambda}$ and $\sigma_{a\lambda}$ are the scattering and absorption coefficients, respectively. To compute the single scattering albedo a Mie code [3] was run for four wavelengths (0.86, 1.65, 2.13 and 3.75 μm) and for r from 5 to 50 μm assuming a gamma size distribution with effective variance 0.1 μm [6]. When the ratio $\omega_{0\lambda}(r)/\omega_{0\lambda}(r_0)$ with $r_0=5$ μm was plotted against $\omega_{0\lambda}(r)$ as a function of the four wavelengths λ, a remarkable linear relationship was discovered:

$$\frac{\omega_{0\lambda}(r)}{\omega_{0\lambda}(r_0)}=p_1\omega_{0\lambda}(r)+p_2. \tag{2}$$

Here slope p_1 and intercept p_2 are wavelength independent parameters. Since $\omega_{0\lambda}(r)=1$ at $\lambda=0.86$ μm for all effective radii r, the sum of p_1 and p_2 is equal to 1; so (2)

* Corresponding author. Tel.: +1 301 614 6122; fax: +1 301 614 6307.
E-mail address: alexander.marshak@nasa.gov (A. Marshak).

0022-4073/$ - see front matter Published by Elsevier Ltd.
doi:10.1016/j.jqsrt.2012.02.021

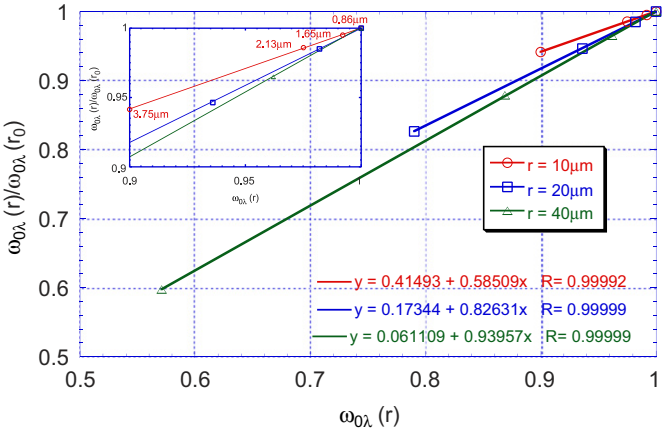

Fig. 1. The single scattering albedo ratio $\omega_{0\lambda}(r)/\omega_{0\lambda}(r_0)$ plotted against $\omega_{0\lambda}(r)$ for four wavelengths λ=0.86, 1.65, 2.13 and 3.75. Single scattering albedos are calculated using Mie theory. Droplet effective radius r=10, 20 and 40 μm; r_0=5 μm. Each colour corresponds to a different value of r. Droplet sizes are assumed to follow a gamma distribution with effective variance v=0.1 μm. Linear fits with regression coefficient R are also shown. The insert zooms the area between 0.9 and 1.

can be rewritten as

$$\frac{\omega_{0\lambda}(r)}{\omega_{0\lambda}(r_0)} = p\omega_{0\lambda}(r)+(1-p). \tag{3}$$

Fig. 1 illustrates Eq. (3) for r=10, 20 and 40 μm and r_0=5 μm. In the next section we provide a simple physical explanation of the spectral invariant relationship (3) and demonstrate its validity for a wide spectral region.

2. Justification of the main results for water droplets

We start with the definition of the single scattering albedo (1). For the visible and near-infrared spectral regions, the scattering efficiency σ_s does not vary much with either wavelength or droplet size; thus we can assume that

$$\sigma_{s\lambda} \approx \sigma_s \pi < r^2 > \tag{4}$$

where σ_s=*const* and $< r^2 >$ is the second moment of the droplet size distribution. To be consistent with notations, we will use symbol $\sigma_{a\lambda}$ for the ratio of the absorption coefficients to $\pi < r^2 >$ through the rest of this paper. In terms of these notations, Eq. (1) can be rewritten as

$$\omega_{0\lambda}(r) = \frac{\sigma_s}{\sigma_s+\sigma_{a\lambda}(r)}. \tag{5}$$

The ratio of $\omega_{0\lambda}$ for two effective radii r and r_0 ($r_0 < r$) will be

$$\frac{\omega_{0\lambda}(r)}{\omega_{0\lambda}(r_0)} = \frac{\sigma_s+\sigma_{a\lambda}(r_0)}{\sigma_s+\sigma_{a\lambda}(r)}. \tag{6}$$

Following Twomey and Bohren [12], for weakly absorbing water droplets

$$1-\omega_{0\lambda}(r) \approx c\sout{\sigma}{}^{k}_{\lambda} r \tag{7}$$

where k_λ is the bulk absorption coefficient (4π multiplied by the ratio of the imaginary part of the refractive index to wavelength). For wavelengths λ between 0.2 and 2.5 μm, the absorption coefficient $10^{-4} < k_\lambda < 10^2$ cm^{-1} ([4], Fig. 2.25, pg. 113). Coefficient c in front of k_λ (equal to 0.85 in [12] for a single droplet) can be well approximated by 2/3 (Frank Evans, personal communication).

Next, since

$$1-\omega_{0\lambda}(r) = \frac{\sigma_{a\lambda}(r)}{\sigma_s+\sigma_{a\lambda}(r)} \tag{8}$$

it follows from Eqs. (7) and (8) that

$$\frac{\sigma_s}{\sigma_{a\lambda}(r)} \approx \frac{\omega_{0\lambda}(r)}{1-\omega_{0\lambda}(r)} = \frac{1-ck_\lambda r}{ck_\lambda r}. \tag{9}$$

Neglecting the second order terms $o[(k_\lambda r)^2]$, we get

$$\sigma_{a\lambda}(r) \approx \sigma_s \frac{ck_\lambda r}{1-ck_\lambda r} = \sigma_s\left[ck_\lambda r+(ck_\lambda r)^2+(ck_\lambda r)^3+\ldots\right] \approx \sigma_s ck_\lambda r. \tag{10}$$

Let us now define a wavelength independent parameter p as

$$p = 1-r_0/r. \tag{11}$$

It follows that

$$r_0 = r(1-p). \tag{12}$$

We now rewrite the ratio (6) as

$$\frac{\omega_{0\lambda}(r)}{\omega_{0\lambda}(r_0)} = \frac{\sigma_s p+\sigma_s(1-p)+\sigma_{a\lambda}(r_0)}{\sigma_s+\sigma_{a\lambda}(r)} = p\omega_{0\lambda}(r)+\frac{\sigma_s(1-p)+\sigma_{a\lambda}(r_0)}{\sigma_s+\sigma_{a\lambda}(r)}. \tag{13}$$

Applying approximation (10) and relationship (12) to the second term in (13) gives

$$\frac{\sigma_s(1-p)+\sigma_{a\lambda}(r_0)}{\sigma_s+\sigma_{a\lambda}(r)} \approx \frac{\sigma_s(1-p)+\sigma_s ck_\lambda r_0}{\sigma_s+\sigma_s ck_\lambda r} = \frac{(1-p)+ck_\lambda r(1-p)}{1+ck_\lambda r} = 1-p. \tag{14}$$

Eq. (14) completes the "proof" of (3) with p defined by (11). Eq. (3) is an approximation but it can be good enough for many purposes. Rearranging Eq. (3) leads to

$$\omega_{0\lambda}(r) = \omega_{0\lambda}(r_0)\frac{1-p}{1-p\omega_{0\lambda}(r_0)}. \tag{15}$$

Eq. (15) states that the single scattering albedo $\omega_{0\lambda}(r)$ can be expressed via one known spectrum $\omega_{0\lambda}(r_0)$. If one knows r and r_0, the slope $p=p(r,r_0)$ can be approximated by Eq. (11). However if r is unknown, p can be obtained directly from Eq. (3). For example, if one knows the two single scattering albedos $\omega_{0\lambda}(r)$ and $\omega_{0\lambda}(r_0)$ at least at one weakly absorbing wavelength, say, $\lambda=2.1$ μm, then p can be determined from Eq. (3) as the slope between two points, one at $\lambda=2.1$ μm and the other at any visible wavelength since $\omega_{0\lambda}(r)=\omega_{0\lambda}(r_0)=1$ there. Knowing p, Eq. (15) provides $\omega_{0\lambda}(r)$ for any wavelength λ if $\omega_{0\lambda}(r_0)$ is available.

How well does Eq. (11) approximate the slope p as a function of r and r_0? Fig. 2 illustrates two slopes: p from the Mie calculations and its approximation $p_{\rm appr}=1-r_0/r$ as a function of r with given $r_0=5$ μm. In spite of a similar shape, there is a substantial difference which is due to approximation (7) and to neglecting the second and higher order terms in (10). (In general, p is a linear function of the ratio r_0/r.) The left panel shows the strong correlation between the two slopes.

3. More wavelengths

As mentioned earlier, Eq. (3) is valid for weakly absorbing wavelengths only. For each droplet effective radius r we define the weakly absorbing wavelengths as ones with $k_\lambda r<0.1$ [thus $(k_\lambda r)^2<0.01$]. For example, for $r=10$ μm, the weakly absorbing wavelengths are the ones with bulk absorption coefficient $k_\lambda<100\ {\rm cm}^{-1}$. The left panel in Fig. 3 illustrates the ratio between two single scattering albedo spectra $\omega_{0\lambda}(r)/\omega_{0\lambda}(r_0)$ for all wavelengths from 0.2 to 4 μm and droplet effective radii: $r=20$ μm, $r_0=10$ μm. In this plot wavelengths are divided into two spectral regions: 0.2 to 2.5 μm (black dots) and 2.5 to 4 μm (grey dots). For the first region $k_\lambda<100\ {\rm cm}^{-1}$ while for the second one $k_\lambda>100\ {\rm cm}^{-1}$ (see the right panel in Fig. 4 adapted from Fig. 2.25 of [4]).

For the weakly absorbing spectral interval (0.2–2.5 μm) the ratio fits a linear function because contributions from the second, $o[(k_\lambda r)^2]$, and higher order terms in (7) and (10) are negligible. The slope of the linear fit $p=0.47$ is close to

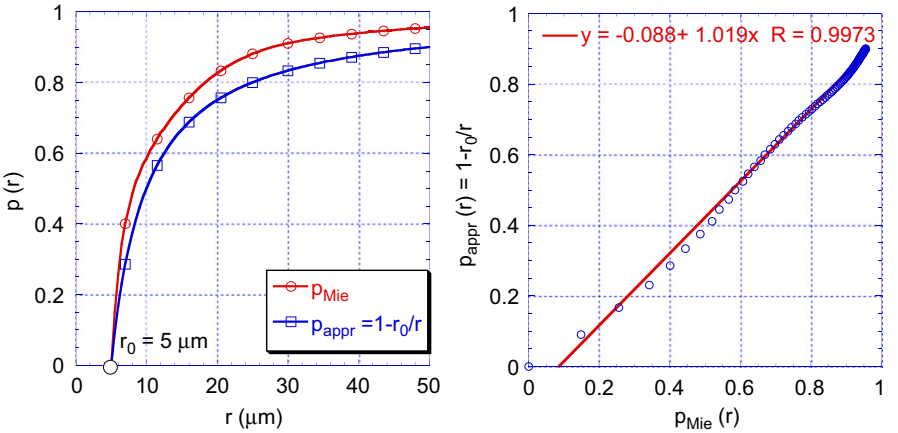

Fig. 2. (**left**) Two slopes $p_{\rm Mie}$ and $p_{\rm appr}$ as a function of r and (**right**) $p_{\rm Mie}$ vs. $p_{\rm appr}$ scatter plot. Slope $p_{\rm Mie}$ is from the Mie calculations using four wavelengths (0.86, 1.65, 2.13 and 3.75 μm) while slope $p_{\rm appr}$ is from Eq. (11) where $r_0=5$ μm.

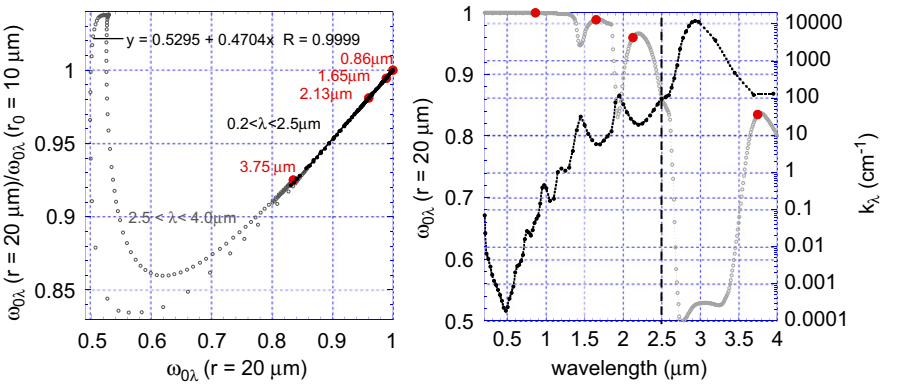

Fig. 3. (**left**) The same as in Fig. 1 but for wavelengths λ between 0.2 μm and 4 μm with 10 nm spectral resolution; $r=20$ μm, $r_0=10$ μm. Grey open dots correspond to wavelengths between 2.5 and 4 μm while black filled dots to wavelengths between 0.2 and 2.5 μm. The linear fit is for the black dots only. Red dots correspond to the four wavelengths (0.86, 1.65, 2.13 and 3.75) used in Fig. 1. (**right**) The single scattering albedo $\omega_{0\lambda}(r)$ for $r=20$ μm (black dots) and the bulk absorption coefficient (grey dots) as a function of wavelength. The bulk absorption coefficient, k_λ, was adapted from Fig. 2.25 of Bohren and Clothiaux [4]. The red dots correspond to the same wavelengths as in left panel. The vertical dash line at 2.5 μm separates two spectral regions. (For interpretation of the references to color in this figure legend, the reader is referred to the web version of this article.)

the one ($p=0.5$) predicted by Eq. (11) with $r=20$ μm and $r_0=10$ μm. We have also added the four wavelengths used in Fig. 1 (red dots). Note that $\lambda=3.75$ μm is just on the edge between the two spectral regions since for water $k_{3.75}=117$ cm^{-1}.

4. Examples for ice crystals

Is Eq. (3) valid for non-spherical ice crystals? To check this we used the single scattering albedo for different types of ice crystals (bullet rosettes, hollow and solid columns, aggregates and plates) provided by Dr. Ping Yang (see [14]). The results are shown in Fig. 4. The regression coefficients R while all above 0.998, are not as good as in the case of spheres (cf. Fig. 1), but the single scattering albedo for the ice crystals exhibits the same spectral invariant behaviour as Eq. (3) predicts.

The bottom right panel of Fig. 4 illustrates that the slopes p can be well approximated by Eq. (11). To get a better linear regression the longer wavelength 3.75 μm was excluded from the slope calculation and only three shorter wavelengths (0.86, 1.65, and 2.13 μm) were used.

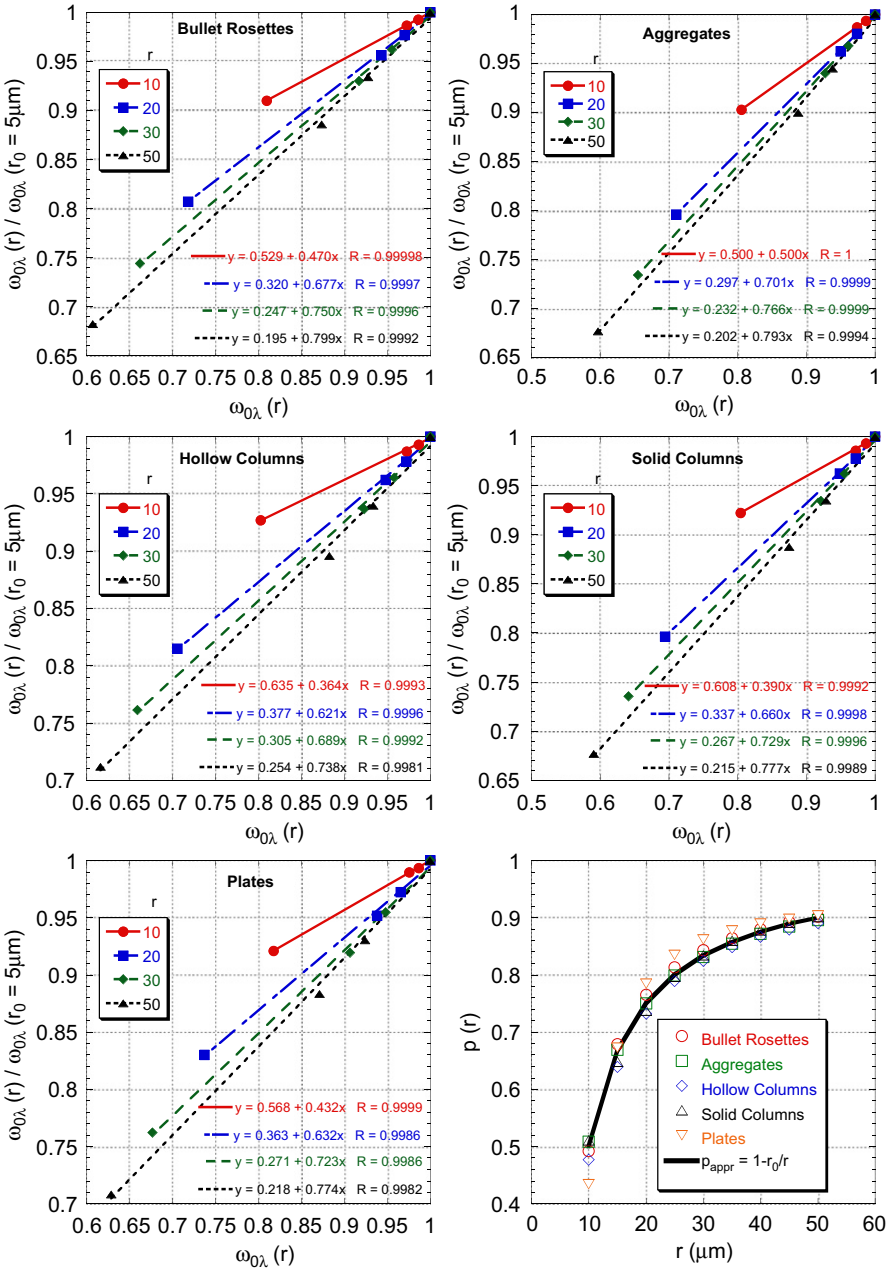

Fig. 4. (**upper 5 panels**) The same as in Fig. 1 but for different ice crystal habits. (**bottom right panel**) Slope p as a function of effective radius r for the ice crystal habits from the upper five panels and the slope p_{appr} is from Eq. (11) where $r_0=5$ μm. Slope p is calculated using only three wavelengths (0.86, 1.65, and 2.13 μm) since the regression is poorer when all 4 wavelengths are used (see text for details).

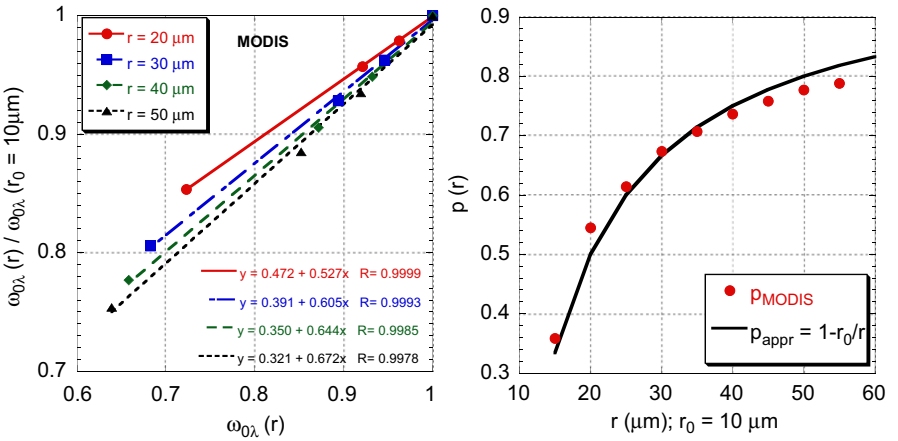

Fig. 5. (**left**) The same as in Fig. 1 but for the MODIS ice model and $r_0=10$ μm. (**right**) The same as the bottom right panel in Fig. 4 but with $r_0=10$ μm. Slope p is calculated using three wavelengths (0.86, 1.65, and 2.13 μm).

As shown in Fig. 3b for water, the bulk absorption coefficient k_λ at $\lambda=3.75$ μm is substantially bigger than that for shorter wavelengths; moreover, the imaginary part of the refractive index for ice at $\lambda=3.75$ μm exceeds almost twice the one for water (e.g., $k_{3.73}=225$ cm^{-1} at temperature of 266 K, see [13]). This causes a poorer regression when all 4 wavelengths were used.

The Moderate Resolution Imaging Spectroradiometer (MODIS) ice models available at 〈http://www.ssec.wisc.edu/~baum/Cirrus/MODIS_V2models.html〉 uses a weighted combination of different ice crystal habits (see [1,2]). For small sizes ($r<30$ μm) MODIS uses 100% droxtals [15] while for sizes between 30 μm and 500 μm, there are 15% of bullet rosettes, 50% solid columns and 35% plates. In Fig. 5 we used crystal sizes from both categories with $r<60$ μm. As Fig. 5 illustrates, the single scattering albedo of the MODIS ice model for weakly absorbing wavelengths also follows the spectral invariant relationship (3) with slope p predicted by Eq. (11) with $r_0=10$ μm and 15 μm $<r<55$ μm.

5. Concluding remarks

It was shown numerically and confirmed theoretically that the spectrum of single scattering albedo $\omega_{0\lambda}(r)$ of water droplets of effective radius r at weakly absorbing wavelengths λ can be well approximated by another spectrum $\omega_{0\lambda}(r_0)$ of effective radius r_0 using Eq. (15) assuming that the slope $p(r,r_0)$ between the ratio $\omega_{0\lambda}(r)/\omega_{0\lambda}(r_0)$ and $\omega_{0\lambda}(r)$ in the linear relationship (3) is known. The slope $p(r,r_0)$ can be approximated by a linear function of r_0/r (see Eq. (11)). In addition to spherical water droplets, it was also shown that the linear relationship (3) (and thus Eq. (15)) is a good approximation for irregular ice crystals of different shapes [14]. For each effective radius r, by weakly absorbing we mean all wavelengths with $k_\lambda r<0.1$ where $k_\lambda=4\pi m_{i\lambda}/\lambda$ is the bulk absorption coefficient ($m_{i\lambda}$ is the imaginary part of the refractive index and λ is wavelength).

The linear relationship (3) and its counterpart (15) allow us to relate radiances as a function of single scattering albedo $\omega_{0\lambda}(r_0)$ to radiances at other single scattering albedos $\omega_{0\lambda}(r)$ in the spectrally invariant relationship between radiances discussed in [10]. This study is yet in progress. The linear relationship (3) also helps to interpret a spectrally invariant relationship in zenith radiances observed near cloud edges [9] and confirmed with intensive radiative transfer calculations [5].

Finally, we note that a spectral invariant relationship for single scattering albedo of green leaves was theoretically predicted by Lewis and Disney [8]. It was found that in the weakly absorbing spectral interval between 710 nm and 790 nm, spectra of green leaves from different species (hazelnut, aspen, jack pine, etc.) were related to one fixed spectrum, called a reference spectrum, via Eq. (13); this property was used in classification of forest types from hyperspectral data [7,11].

Acknowledgements

This research was supported by the Office of Science (BER, US Department of Energy, Interagency Agreement No. DE-AI02-08ER64562) as part of the ASR programme. We also thank Drs. F. Evans, P. Gabriel, R. Kahn, A. Lyapustin, V. Martins, T. Varnai, Z. Zhang for fruitful discussions. We are grateful to Dr. P. Yang for providing a database which gives the phase function for individual ice crystals, to Dr. Y. Yang for his help with Mie calculations and to Dr. Clothiaux for providing data for Fig. 2.25 from Bohren and Clothiaux [4].

References

[1] Baum BA, Heymsfield AJ, Yang P, Bedka ST. Bulk scattering properties for the remote sensing of ice clouds. Part I: Data and models. J Appl Meteorol 2005;44:1885–95.
[2] Baum BA, Yang P, Heymsfield AJ, Platnick S, King MD, Hu Y-X, et al. Bulk scattering properties for the remote sensing of ice clouds. Part II: Narrowband models. J Appl Meteor 2005;44:1896–911.
[3] Bohren CF, Huffman DR. Absorption and scattering of light by small particles. New York: J. Wiley & Sons; 1983 530 pp.

[4] Bohren CF, Clothiaux DR. Fundamentals of atmospheric radiation. Weinheim: J. Wiley-VCH Verlag GmbH & Co. KGaA; 2006 472 pp.
[5] Chiu JC, Marshak A, Knyazikhin Y, Wiscombe WJ. Spectrally-invariant behavior of zenith radiance around cloud edges simulated by radiative transfer. Atmos Chem Phys 2010;10:11295–303.
[6] Hansen JE, Travis LD. Light scattering in planetary atmospheres. Space Sci Revi 1974;16:527–609.
[7] Knyazikhin Y, Schull MA, Xu L, Myneni RB, Samanta A. Canopy spectral invariants. Part 1: A new concept in remote sensing of vegetation. J Quant Spectrosc Radiat Transfer 2011;112:727–35.
[8] Lewis P, Disney M. Spectral invariants and scattering across multiple scales from within-leaf to canopy. Remote Sens Environ 2007;109:196–206.
[9] Marshak A, Knyazikhin Y, Chiu JC, Wiscombe WJ. Spectral invariant behavior of zenith radiance around cloud edges observed by ARM SWS. Geophys Res Lett 2009;36:L16802, doi:10.1029/2009GL039366.
[10] Marshak A, Knyazikhin Y, Chiu C, Wiscombe W. Spectrally-invariant approximation within atmospheric radiative transfer. J Atmos Sci 2011;68:3094–111.
[11] Schull MA, Knyazikhin Y, Xu L, Samanta A, Carmona PL, Lepine L, et al. Canopy spectral invariants, Part 2: Application to classification of forest types from hyperspectral data. J Quant Spectrosc Radiat Transfer 2011;112:736–50.
[12] Twomey S, Bohren CF. Simple approximations for calculations of absorption in clouds. J Atmos Sci 1980;37:2086–94.
[13] Warren SG, Brandt RE. Optical constants of ice from the ultraviolet to the microwave: a revised compilation. J Geophys Res 2008: 113, doi:10.1029/2007JD009744.
[14] Yang P, Liou KN, Wyser K, Mitchell D. Parameterization of the scattering and absorption properties of individual ice crystals. J Geophys Res 2000;105:4699–718.
[15] Yang P, Baum BA, Hemsfield AJ, Hu Yong X, Huang H-L, Tsay S-C, et al. Single-scattering properties of droxtals. J Quant Spectrosc Radiat Transfer 2003;79-80:1159–69.